

## Print Localization on Transparent Pharmaceutical Capsules

Andraž Mehle<sup>1</sup>, Marko Bukovec<sup>1</sup>, Franjo Pernuš<sup>1,2</sup>, Boštjan Likar<sup>1,2</sup>, and Dejan Tomaževič<sup>1,2</sup>

<sup>1</sup>Sensum, Computer Vision Systems  
Ljubljana, Slovenia

<sup>2</sup>Faculty of Electrical Engineering,  
University of Ljubljana, Slovenia  
andraz.mehle@sensum.eu

**Abstract** *This paper presents a novel method for real-time print localization on transparent pharmaceutical capsules which is a crucial step for automated visual inspection. The method is based on print segmentation and template matching technique. A print appearance used for template matching is constructed from capsule images without defects during the training phase. Print localization during inspection phase is achieved by combination of phase correlation between template and sample, and additional criterion to compensate for print overlaps and ambiguities due to capsule's transparency. The method was evaluated in terms of robustness, accuracy and speed on a large image database of transparent capsules with radial print. Results were compared to the method for standard opaque capsules. The results indicate that our method shows improved robustness and accuracy. Moreover, computational time of less than 10 milliseconds allows real time visual inspection of pharmaceutical capsules.*

### 1 Introduction

Nowadays, pharmaceutical industry produces vast amount of different pharmaceutical tablets and capsules. To avoid dangerous drug mix-ups, every type of product has to be quickly, easily and unambiguously identified by doctors and pharmacists as well as by end consumers. Different products should be uniquely characterized by their size, shape, color, texture, prints, etc. [1]. Demands are enforced by national regulators in each country such as a regulation code 21CFR206 [7] issued by the Food and Drug Administration in USA. Besides unambiguous identification, high quality of visual appearance of pharmaceutical products is required by pharmaceutical companies since defected products cause doubts and lower level of trust among consumers.

The most common method for visual quality control of pharmaceutical capsules is manual inspection by various methods. The disadvantage of such methods is that the overall quality of the whole batch of capsules is estimated by inspecting only certain sample of capsules. The required quality of single product can thus not be guaranteed. Furthermore some countries, e.g. Japan, have regulations that enforce every single product to be visually inspected, either manually or automatically. The capsules may be inspected

before or after they have been filled with active substance, however the latter is more common. Since manual visual inspection is slow, unreliable, tedious, costly and even harmful to the operators, fully automated visual inspection of every single product in a batch is emerging.

Automated visual inspection of pharmaceutical capsules [10, 12] is very challenging, because capsules come in different sizes, colors and prints and may have various visual defects. Sophisticated high-tech machine vision system with fast mechanical capsule manipulation, proper illumination, fast image acquisition, image analysis, capsule classification and sorting mechanism is thus required [3]. Speed requirements of such systems are from 20 up to 100 products per second. This calls for fast and efficient image processing algorithms with low computational complexity but high reliability and robustness [8, 14].

Beside other visual characteristics, print plays important role in identification of pharmaceutical capsules, because it provides fast identification of manufacturer and active substance [17]. Print can include company logo or name, commercial name of the product, chemical name or even information about dosage. Print on pharmaceutical capsules consists of two parts, one on each half of a capsule. Print can be oriented along the main axis of the capsule, i.e. axial print, or perpendicular to the main axis, i.e. radial print. Combination of axial and radial print is also possible, wherein each part of a capsule has different print orientation [15]. Print legibility is the most important criterion for identification. Despite optimal choice of print size, shape and content, print defects made during printing process or transportation, may affect print legibility. The defects include partly or entirely missing print, multiple prints, blurred print, smudged print, ink spots, color and size variations of the print, etc.

Capsules with transparent shell are commonly used as the dose-holding system for breath-actuated dry powder inhalers [6], devices for delivery of drugs to the lung. Many disorders affecting the lungs such as asthma are treated by inhaling drugs to increase the airflow or reduce inflammation. Transparency of capsule's shell allows the user to see the active substance (powder) and to easily check if the whole dose was properly inhaled. Capsules may be completely clear (natural gelatin color) or colored and may include prints.

There are various automated visual inspection systems for pharmaceutical capsules on the market from companies such as Ackley, Eisai, Ikegami, Mutual, Proditex, Seidenader, Sensum and Viswill but only a few research articles on this subject have been published so far. Karloff et al. [10] and Islam et al. [8, 9] designed a low cost capsule inspection system that can be integrated into an existing mechanical capsule sorters. The system is capable of inspecting 20 capsules per second and is able to inspect uni-color, bi-color as well as transparent capsules. However, their system can only detect larger defects such as cracks, dents, double caps and improper length and can only inspect capsules without print. Visual inspection of printed capsules is even more challenging task. The main problem is cylindrical shape, which allows capsules to freely rotate around their main axis. Thus, the spatial location of a print may vary from image to image, where portions of a print may be hidden. Moreover, due to the cylindrical shape of capsules, spatial distortions occur when 3D capsule surface is projected onto 2D image plane. Distortions are most prominent at the border of a capsule.

Print localization is a crucial element of automated visual inspection of printed capsules, without which further analysis and classification is not possible. The area of capsule's surface containing print is inspected separately from the rest of a capsule. Successful print localization enables inspection of print quality as well as inspection of the rest of a capsule. If the print is not properly localized, portions of print may be recognized as defects. Špiclin et al. [14] proposed a template matching technique for localization of print on opaque capsules. They eliminated spatial distortions by transforming a capsule image into cylindrical coordinate system and used template matching technique [16] to localize print. A print appearance template is constructed from capsule images without defects during the training phase. Because of high speed requirements, registration method incorporates simple two dimensional translation as transformation model between template and sample image. In general, transformation is not linear due to different spatial deformations that can occur during printing process or additional distortions caused by imperfect image acquisition.

Transparent capsules bring additional challenges to all segments of automated visual inspection including print localization. Transparency causes that both the front surface, i.e. capsule surface faced towards the camera (foreground), and the back surface, i.e. capsule surface faced to the opposite direction (background), are captured (Fig. 1). When a print is located on the background, it appears mirrored and has lower contrast. Moreover, portions of the print can be concurrently visible on the foreground and on the background and may overlap. Furthermore, spatial deformations due to printing process and distortions due to imperfect image acquisition are emphasized. Axial capsule movement during printing process causes radial line to manifest as helix (Fig. 1, left), while slightly tilted capsule causes radial line to be seen as ellipse (Fig. 1, right).

Due to problems mentioned above, the template matching method described by Špiclin et al. [14] does not achieve adequate results. In this paper we propose a method for real-time localization of print on transparent capsules that is ca-

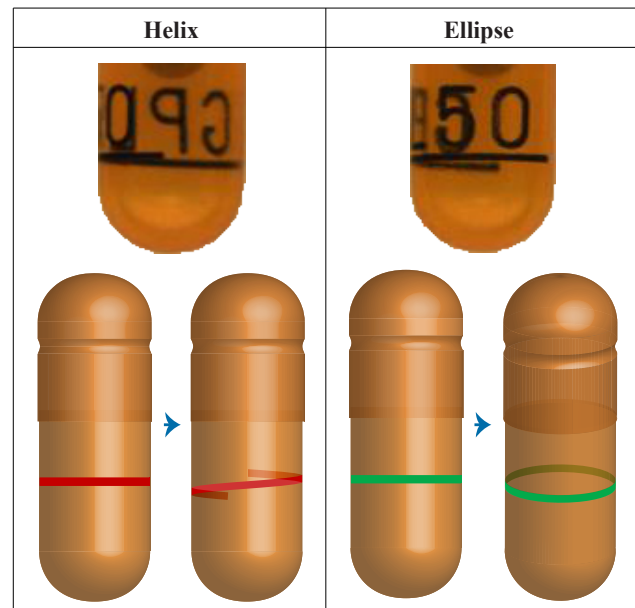


**Figure 1:** Spatial deformations of print on transparent capsules: altered camera viewing angle causes radial line to manifest as ellipse (left), rotated radial line manifests as helix.

pable of matching both foreground and background print simultaneously and is robust to spatial deformations and distortions. We validated our method in terms of robustness, accuracy and speed on a large image database of transparent capsules with radial print.

## 2 Materials and Methods

In this section the method for print localization on transparent pharmaceutical capsules is described. The method matches a print template to foreground and background print on sample image where foreground and background print may overlap significantly (Fig. 2). Our method is based on segmented print images.

First the entire capsule is segmented by border tracking algorithm [13] (Fig. 2, left). Then the print is segmented from color image by max shift segmentation algorithm [5] (Fig. 2, right) which is based on mean shift clustering [4]. The task of max shift segmentation algorithm is to separate the modes of the probability distribution in multidimensional histogram, i.e. to separate clusters in feature space of a histogram that represent different regions in an image. Color values of image pixels are mapped into a 3D histogram, a feature space with multivariate and generally multi-modal probability distribution. The regions in histogram with the highest density correspond to clusters centered on the modes of the underlying probability distribution. Max shift algorithm uses a cube search kernel to find the clusters in the histogram. In each iteration the kernel is shifted in the direction of maximum gradient inside the kernel. The center of a cluster is obtained by convergence of the kernel from the initial location. Once the center is obtained, the corresponding feature points that belong to this cluster are determined by applying the max shift algorithm to the neighboring points of the cluster center. The procedure is

repeated until all the feature points are labeled.

Main axis of the capsule is estimated from the capsule's shape obtained from capsule segmentation and is used for transformation into cylindrical coordinate system as described in [14], where only capsule region where print presence is expected is transformed (Fig. 3a).



**Figure 2:** Segmented color image (left) and corresponding print segmentation (right) with print regions (rectangles).

Špiclin et al. [14] performed transformation of print region into cylindrical coordinate system only for visible (foreground) print, i.e. transformation was performed only on the interval of  $[0^\circ, 180^\circ]$ . In contrast, for transparent capsules both foreground and background print are visible but inseparable, thus the extended transformation (from  $0^\circ$  to  $360^\circ$ ) is performed (Fig. 3a). Transformation of print on interval  $[0^\circ, 180^\circ]$  can be interpreted as foreground print with visible background, while transformation on interval  $[180^\circ, 360^\circ]$  represents background print occluded by foreground. The goal of the method is to match the entire  $360^\circ$  template to foreground and background print.

The template is matched to the input image by calculating phase correlation [11] between template  $h(x, y)$  and input image  $f(x, y)$ . Phase correlation method is based on Fourier Shift Theorem [2] and can be efficiently calculated in frequency (Fourier) domain. It computes normalized cross-power spectrum  $S(\xi, \eta)$  between images:

$$S(\xi, \eta) = \frac{F(\xi, \eta)H^*(\xi, \eta)}{|F(\xi, \eta)H^*(\xi, \eta)|}, \quad (1)$$

$$PC(u, v) = \mathcal{F}^{-1}\{S(\xi, \eta)\}, \quad (2)$$

where  $H(\xi, \eta)$  and  $F(\xi, \eta)$  are discrete 2D Fourier transforms of template and input image respectively and  $H^*$  is complex conjugate of  $H$ .  $PC(u, v)$  denotes inverse Fourier transform of  $S(\xi, \eta)$  which is ideally (according to Fourier Shift Theorem) a Dirac delta function  $\delta(x + u_0, y + v_0)$  centered at  $(u_0, v_0)$ , where  $u_0$  and  $v_0$  represent shift between images. The problem of finding shift  $(u_0, v_0)$  thus translates to the problem of locating delta peak in  $PC$ :

$$(u_0, v_0) = \underset{(u, v)}{\operatorname{argmax}}(PC(u, v)). \quad (3)$$

Phase correlation shows strong robustness against the narrow band noise and non-uniform illumination changes [11, 18].

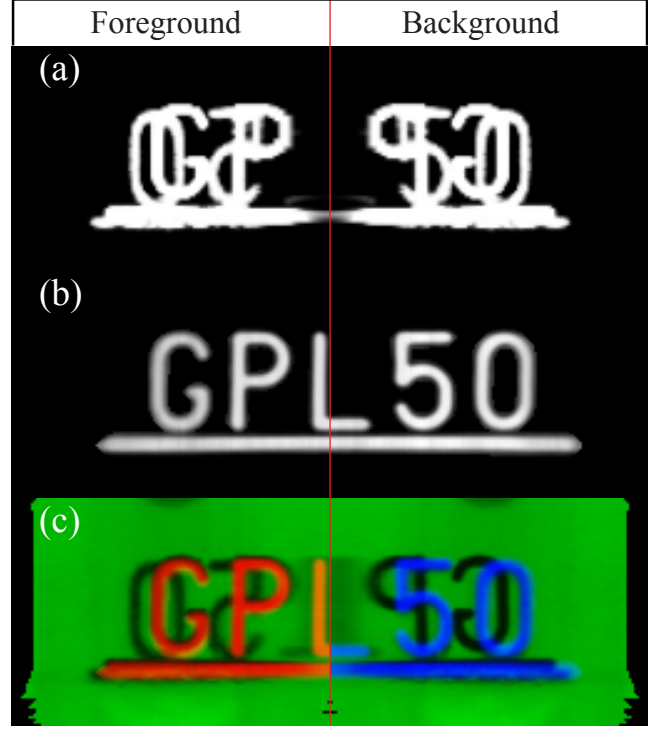


**Figure 3:** (a)  $360^\circ$  input image, (b) template image, (c) template image matched to input image (red - foreground, blue - background).

Because of foreground and background print overlap, and due to similar appearance of individual symbols or characters, phase correlation often results into more than one distinct peak, where the most prominent one does not necessarily represents the optimal alignment (Fig. 4). Therefore, additional criterion is needed to isolate the optimal peak from  $N$  most distinct peaks  $(u_i, v_i; i = 1 \dots N)$ .

Let us define Foreground-Background Overlap

$$FBO_{u_i, v_i} = FO_{u_i, v_i} + BO_{u_i, v_i}, \quad (4)$$

that measures overlap of print area between template and input image separately for foreground ( $FO$ ) and background ( $BO$ ) at given shift  $(u_i, v_i)$ . Each of  $N$  most distinct peaks  $(u_i, v_i; i = 1 \dots N)$  can further be evaluated as

$$C_{u_i, v_i} = PC_{u_i, v_i} FBO_{u_i, v_i}, \quad (5)$$

where  $PC_{u_i, v_i}$  represents the value of  $PC$  (2) at given peak location  $(u_i, v_i)$ . The optimal alignment, i.e. the shift between the template and input image, is found as

$$(u_0, v_0) = \underset{i}{\operatorname{argmax}}(C_{u_i, v_i}). \quad (6)$$

The goal of  $FO$  is to measure the overlap between the template and input image only on foreground (from  $0^\circ$  to  $180^\circ$ ). It is defined as:

$$FO_{u_i, v_i} = \left[ \frac{\sum_{x, y} f_{fg} h_{fg}}{\sum_{x, y} h_{fg}} \right] \sum_{x, y} f_{fg} h_{fg} \quad (7)$$

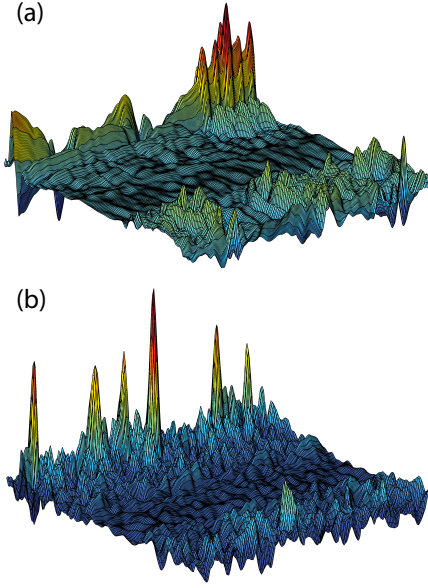


**Figure 4:** Examples of  $PC$  correlation images with several distinct peaks: (a) cap print correlation image, (b) body print correlation image.

Input image  $f_{fg}$  represents only foreground half of  $360^\circ$  input image (Fig. 5c):

$$f_{fg} = f(x, y) m(x, y), \quad (8)$$

where mask  $m(x, y)$  (Fig. 5b) is equal to one at the foreground (interval from  $0^\circ$  to  $180^\circ$ ) and zero elsewhere. Similarly, template  $h_{fg}$  represents only foreground half of the template at given shift  $(u_i, v_i)$  (Fig. 5e):

$$h_{fg} = h(x + u_i, y + v_i) m(x, y). \quad (9)$$

The first term of  $FO$  (7) represents the overlap factor, i.e. fraction of template  $h_{fg}$  overlapped with input  $f_{fg}$ . The overlap factor is equal to one when the entire foreground template  $h_{fg}$  is overlapped with  $f_{fg}$  and zero when they are completely mismatched. The second term in expression (7) stands for size of overlap region. Therefore measure  $FO$  has the highest value when the entire foreground template  $h_{fg}$  is overlapped (first term of (7)) and it overlaps as much input  $f_{fg}$  as possible (second term of (7)). When background print dominates on  $f_{fg}$  the  $FO$  might be highest at shifts where foreground template overlaps with background print, especially if the print appearance is very symmetrical. Thus an additional complementary measure of background overlap ( $BO$ ) is needed.

Similarly to  $FO$  the  $BO$  is defined as:

$$BO_{u_i, v_i} = \left[ \frac{\sum_{x, y} f_{bg} h_{bg}}{\sum_{x, y} f_{bg}} \right] \sum_{x, y} f_{bg} h_{bg} \quad (10)$$

New input images  $f_{bg}$  and  $h_{bg}$  are defined by erasing the overlapping print on  $f_{fg}$  and  $h$  respectively (Fig. 5d and 5f):

$$f_{bg} = f_{fg} (1 - h_{fg}), \quad (11)$$

$$h_{bg} = h_F (1 - h_{fg}) m, \quad (12)$$

where  $h_F$  is vertically flipped background part of the template. At optimal shift  $(u_0, v_0)$   $f_{bg}$  represents only the background print since the foreground print has been erased (11). Similarly from  $h_F$ , i.e. the part of the template expected on the background, the foreground part of the template ( $h_{fg}$ ) has been erased (12), because the background print is always occluded with foreground print. While  $FO$  measures an overlap between foreground print  $f_{fg}$  and foreground template  $h_{fg}$ ,  $BO$  measures an overlap between the rest of visible print ( $f_{bg}$ ) and expected template on the background  $h_{bg}$ .

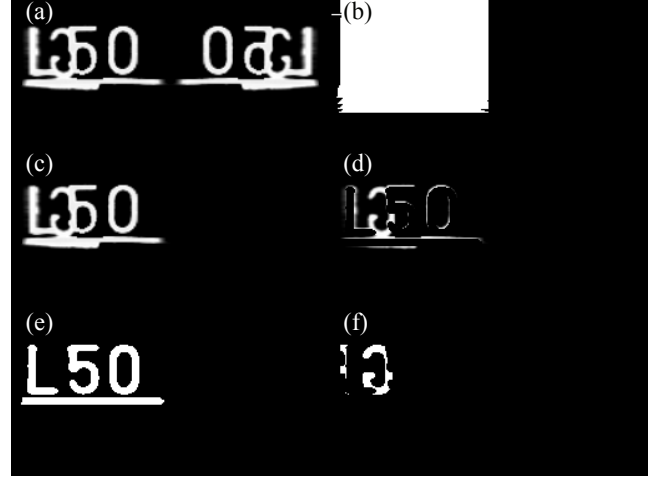


**Figure 5:** Input images for calculation of  $FO$  and  $BO$ : (a)  $360^\circ$  input image  $f(x, y)$ , (b) mask image  $m(x, y)$ , (c) foreground print  $f_{fg}$ , (d) background print  $f_{bg}$ , (e) foreground template  $h_{fg}$ , (f) background template  $h_{bg}$ .

### 3 Experiments and Results

Performance of the proposed method was evaluated in terms of robustness, accuracy and speed on a database of 516 images of transparent orange capsules with radial print on cap and body. The cap print included radial line with company logo while the body print included radial line and some text. The template and input image size was  $256 \times 128$  pixels. Gold standard of print locations was obtained by manually determining three pairs of corresponding points between template and each input image. The localization error after the matching was defined as RMS of corresponding point distances. The implementation of the method was done in C++ and executed on a 3.4 GHz Intel Core i7 3770 platform. Speed was measured by the mean execution time to assess the feasibility of the method for real-time visual inspection of pharmaceutical capsules. The performance was compared to the print localization method for opaque capsules proposed by Špiclin et al. [14] where template matching technique based on normalized cross-correlation ( $NCC$ ) was used. The spatial deformations of the print in cylindrical coordinate system can be as large as 5 pixels thus the localization was considered successful if the error was below 5 pixels. The accuracy was defined as mean error of all successful print localizations. The performance of the two methods is presented in Table 1. Additionally,

Method	Cap print		Body print	
	NCC	PC FBO	NCC	PC FBO
Robustness (%)	91.8	99.1	98.6	100
Accuracy (pixel)	1.9	1.4	1.8	1.1
Speed (ms)	4	7	4	7

**Table 1:** Performance of the proposed method (PC FBO) and method for opaque capsules (NCC) [14] in terms of robustness (percentage of successful localizations), accuracy (mean error of successful localizations in pixels), and speed (mean computation time in milliseconds).

Fig. 6 shows cumulative fraction of matched samples with respect to print localization error. Fig. 7 shows an example of failure of the print localization method for opaque capsules and successful print localization of the same sample with the proposed method.

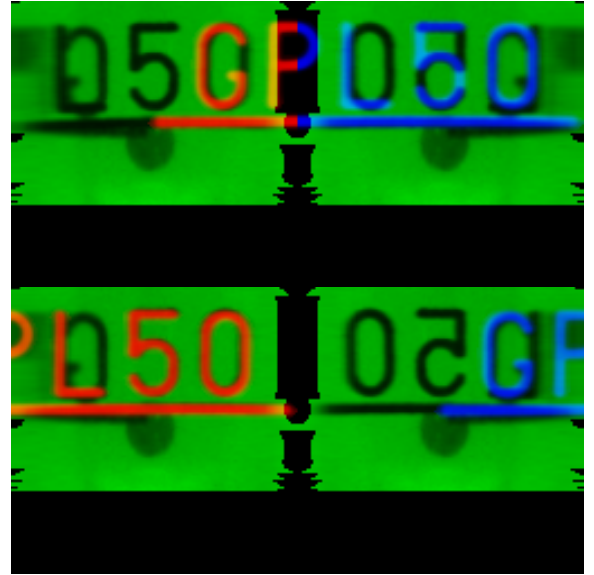


**Figure 7:** An example of unsuccessful print localization with NCC (top) and successful print localization with PC FBO (bottom). The print template is colored red on the foreground (from 0° to 180°) and blue on the background (from 180° to 360°). Similarity between characters and overlapping of foreground and background print caused localization with NCC to fail.

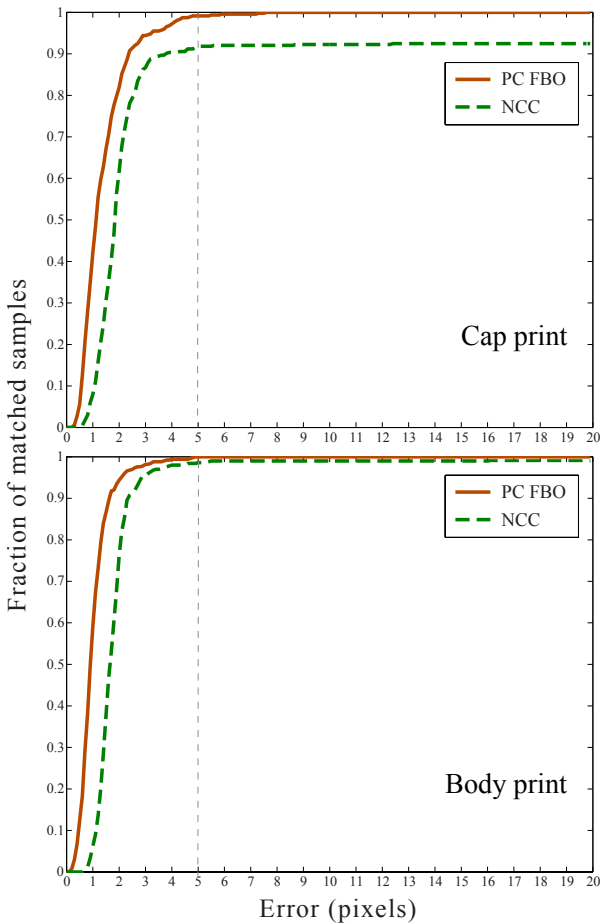


**Figure 6:** Cumulative fraction of matched samples with respect to print localization error for cap print (top) and body print (bottom). Our method (PC FBO) is compared to the method for opaque capsules (NCC) [14]. Localization with error less than 5 pixels was considered successful.

## 4 Discussion and Conclusion

Successful print localization is a crucial element of visual inspection of pharmaceutical capsules with print. It allows proper inspection of print validity as well as detection of defects on the rest of the capsule’s surface. A novel method for print localization on transparent capsules was proposed. The method was evaluated on real images and showed sufficient performance for defect detection and print quality inspection. The method shows high robustness to illumination changes, small spatial deformations of the print, and overlapping of foreground and background print. The method was compared to the print localization method used for standard opaque capsules where only foreground print is visible.

The success rate of our method was 99.1 % for the cap print and 100 % for the body print while the standard method with NCC achieved 91.8 % and 98.6 % success rate respectively. Our method shows great improvement of cap print localization. Extremely symmetrical appearance and small size of cap print made its localization much more difficult than that of the body print. Furthermore the standard method often resulted in completely false localization where the foreground template was matched to the background print or vice versa. The maximum error of our method was 7.6 pixels which is only a few pixels above the threshold of successful localization. Our method is computationally almost two times more demanding than the standard method but shows highly improved robustness and accuracy. Furthermore the execution time of 7 milliseconds for one image is sufficient for real time visual inspection of pharmaceutical capsules.

The overall measure  $C_{u_i, v_i}(5)$  is only as precise as  $PC$  because  $FBO$  only selects the optimal peak among  $N$  peaks

of  $PC$ . Furthermore if  $N$  is too low, none of the peaks might represent optimal shift. To achieve better precision and robustness we can calculate the measure  $FBO$  at all possible shifts ( $u_i = 0 \dots W - 1, v_i = 0 \dots H - 1$ ) where  $W$  is the width and  $H$  is the height of the input image. Calculating the entire  $FBO$  in time domain is computationally very expensive but it turns out that it can be efficiently calculated in Fourier domain in real time.

Because of high speed requirements the assumed transformation between template and input image was simple translation. However spatial deformations of the print caused the localization error to be as large as 5 pixels on some parts of the print. That means that during inspection phase the print template had to be substantially dilated in order to entirely cover the print. Our future work includes the calculation of the entire  $FBO$  in Fourier domain, the modeling of the most significant spatial deformations of the print, and the estimation of non-rigid transformation that will eliminate spatial deformations (ellipse and helix) on each sample image.

## Acknowledgement

This work was supported by the Ministry of Higher Education, Science and Technology, Republic of Slovenia under grants L2-4072, L2-5472, by Sensum, Computer Vision Systems, and by the European Union, European Social Fund.

## References

- [1] Adrienne Berman. Reducing medication errors through naming, labeling, and packaging. *Journal of Medical Systems*, 28(1):9–29, Feb. 2004.
- [2] Ronald N. Bracewell. *The Fourier Transform and Its Applications*. McGraw-Hill Higher Education, 2000.
- [3] Marko Bukovec, Ziga Spiclin, Franjo Pernus, and Bostjan Likar. Automated visual inspection of imprinted pharmaceutical tablets. *Measurement Science & Technology*, 18(9):2921–2930, Sept. 2007.
- [4] Yizong Cheng. Mean shift, mode seeking, and clustering. *IEEE Transactions on Pattern Analysis and Machine Intelligence*, 17(8):790–799, 1995.
- [5] J. Derganc, B. Likar, and F. Pernus. Shading correction and segmentation of color images. In *Proceedings of the 2nd International Symposium on Image and Signal Processing and Analysis, 2001. ISPA 2001*, pages 345–350, 2001.
- [6] David Edwards. Applications of capsule dosing techniques for use in dry powder inhalers. *Therapeutic delivery*, 1(1):195–201, July 2010.
- [7] FDA. Code of federal regulations (21CFR206) imprinting of solid oral dosage form drug products for human use. <http://www.accessdata.fda.gov/>.
- [8] M.J. Islam, M. Ahmadi, and M.A. Sid-Ahmed. Image processing techniques for quality inspection of gelatin capsules in pharmaceutical applications. In *10th International Conference on Control, Automation, Robotics and Vision, 2008. ICARCV 2008*, pages 862–867, Dec. 2008.
- [9] M.J. Islam, S. Basalamah, M. Ahmadi, and M.A. Sid-Ahmed. Capsule image segmentation in pharmaceutical applications using edge-based techniques. In *2011 IEEE International Conference on Electro/Information Technology (EIT)*, pages 1–5, May 2011.
- [10] A.C. Karloff, N.E. Scott, and R. Muscedere. A flexible design for a cost effective, high throughput inspection system for pharmaceutical capsules. In *IEEE International Conference on Industrial Technology, 2008. ICIT 2008*, pages 1–4, Apr. 2008.
- [11] CD Kuglin and DC Hines. The phase correlation image alignment method. *IEEE Conference on Cybernetics and Society*, pages 163–165, 1975.
- [12] Elias N Malamas, Euripides G.M Petrakis, Michalis Zervakis, Laurent Petit, and Jean-Didier Legat. A survey on industrial vision systems, applications and tools. *Image and Vision Computing*, 21(2):171–188, Feb. 2003.
- [13] Miha Možina, Dejan Tomažević, Franjo Pernuš, and Boštjan Likar. Real-time image segmentation for visual inspection of pharmaceutical tablets. *Machine Vision and Applications*, 22(1):145–156, Jan. 2011.
- [14] Z. Špiclin, B. Likar, and F. Pernuš. Real-time print localization on pharmaceutical capsules for automatic visual inspection. In *2010 IEEE International Conference on Industrial Technology (ICIT)*, pages 279–284, Mar. 2010.
- [15] Fridrun Podczeck and Brian E. Jones. *Pharmaceutical Capsules*. Pharmaceutical Press, 2004.
- [16] D. M. Tsai and C. T. Lin. Fast normalized cross correlation for defect detection. *Pattern Recognition Letters*, 24(15):2625–2631, Nov. 2003.
- [17] P. Vasudevan, T. DelGianni, and W. O. Robertson. Avoiding medication mixups - identifiable imprint codes. *Western Journal of Medicine*, 165(6):352–354, Dec. 1996.
- [18] Barbara Zitová and Jan Flusser. Image registration methods: a survey. *Image and Vision Computing*, 21(11):977–1000, Oct. 2003.